Lung dysfunction causes systemic hypoxia in estrogen receptor β knockout (ER$\beta^{-/-}$) mice

Andrea Morani*, Rodrigo P. A. Barros*†, Otabek Imamov*, Kjell Hultenby‡, Anders Arner§, Margaret Warner*, and Jan-Åke Gustafsson*¶

*Department of Biosciences and Nutrition and ‡Clinical Research Centre, Karolinska Institute, Novum, S-141 86 Huddinge, Sweden; †Department of Physiology and Biophysics, Institute of Biomedical Sciences, University of São Paulo, Av. Prof. Lineu Prestes, 1524, 05508-900, São Paulo, Brazil; and §Department of Physiology and Pharmacology, Karolinska Institute, Solna Campus, SE-171 77 Stockholm, Sweden

Contributed by Jan-Åke Gustafsson, March 17, 2006

Estrogen receptor β (ERβ) is highly expressed in both type I and II pneumocytes as well as bronchiolar epithelial cells. ERα is not detectable in the adult lung. Lungs of adult female ERβ knockout (ER$\beta^{-/-}$) mice have already been reported to have fewer alveoli and reduced elastic recoil. In this article, we report that, by 5 months of age, there are large areas of unexpanded alveoli in lungs of both male and female ER$\beta^{-/-}$ mice. There is increased staining for collagen and, by EM, abnormal clusters of collagen fibers are seen in the alveolar septa of ER$\beta^{-/-}$ mice. Immunohistochemical analysis and Western blotting with lung membrane fractions of ER$\beta^{-/-}$ mice revealed down-regulation of caveolin-1, increased expression of membrane type-1 metalloproteinase, matrix metalloproteinase 2 (active form), and tissue inhibitors of metalloproteinases 2. Hypoxia, measured by immunohistochemical analysis for hypoxia-inducible factor 1α and chemical adducts (with Hypoxyprobe), was evident in the heart, ventral prostate, perioovarian sac, kidney, liver, and brain of ER$\beta^{-/-}$ mice under resting conditions. Furthermore, both male and female adult ER$\beta^{-/-}$ mice were reluctant to run on a treadmill and tissue hypoxia became very pronounced after exercise. We conclude that ERβ is necessary for the maintenance of the extracellular matrix composition in the lung and loss of ERβ leads to abnormal lung structure and systemic hypoxia. Systemic hypoxia may be responsible for the reported left and right heart ventricular hypertrophy and systemic hypertension in ER$\beta^{-/-}$ mice.

extracellular matrix | caveolin | metalloproteinase | hypertension | lung fibrosis

The importance of estrogens in development, physiology, and pathology of the lung has been known for some time. Estrogen hastens the onset of surfactant production and influences alveolar size and number. In fact, there is sexual dimorphism in late gestational and postnatal maturation of the lung in mammals (1, 2). The lack of detectable estrogen receptor α (ERα) in the lung led to the belief that effects of estrogen on the lung were indirect. It was not until the discovery of ERβ in 1995 (3) that it became clear that estrogen, acting through ERβ, has direct actions on the lung. ERβ knockout (ER$\beta^{-/-}$) mice (4) are characterized by right and left ventricle hypertrophy (5), systemic hypertension (6), ovarian dysfunction (7), and incompletely differentiated epithelium in ventral prostate (8), mammary gland (9), and colon (10). Compared with their WT littermates, female ER$\beta^{-/-}$ mice are reported to have fewer alveoli (11), reduced lung volume at a transpulmonary pressure of 20 cm of H_2O and reduced elastic recoil (12). Massaro *et al.* (12) attributed the lung phenotype to some defect of the extracellular matrix (ECM) composition. ECM is essential for normal tissue development, homeostasis, and wound repair. Physiologically, there is a balance between matrix protein accumulation and degradation. The ECM is composed of collagenous and noncollagenous proteins in which turnover is predominantly regulated by a family of enzymes called matrix metalloproteinases (MMPs). Recent data have revealed a major role for MMPs in normal lung development and maintenance of lung architecture (13–17). Despite their key role in repair of the lung, MMPs can lead to destruction of alveolar epithelium, and overactivity of MMPs in the lung is thought to contribute to pulmonary diseases such as emphysema, idiopathic interstitial pneumonias, chronic obstructive pulmonary disease, and chronic reactive airway disease (18–21). MMPs are also involved in the invasion process of several metastatic cancer cells. The tissue inhibitors of metalloproteinases (TIMPs) are established endogenous inhibitors of MMPs. TIMP2 can bind to cell surface membrane type-1 metalloproteinase (MT1-MMP) to act as a "receptor" for pro-MMP2. The proteolytic modification of MMP2 from an inactive 72-kDa protein to a 62-kDa active form is catalyzed by MT1-MMP in association with TIMP2 (22).

MT1-MMP associates with caveolin-1 in lipid rafts on the cell surface. Expression of caveolin-1 does not affect the MT1-MMP-dependent activation of pro-MMP2, but there is evidence that caveolar localization of MT1-MMP inhibits MT1-MMP-dependent cell migration in several kinds of cancer (23). Caveolin-1 plays an essential role in caveolar formation (24). Lungs of caveolin-1 knockout mice are fibrotic with accumulation of ECM and fibroblast proliferation in the alveolar septa (25). Caveolin-1 is ERβ-regulated in skeletal muscle (26), and the lungs of caveolin-1$^{-/-}$ mice bear some resemblance to lungs of ER$\beta^{-/-}$ mice.

In the present study, we investigated the pathological phenotype of the lung in ER$\beta^{-/-}$ mice. We report that, after 5 months of age, lungs of both male and female ER$\beta^{-/-}$ mice are fibrotic with large regions of unexpanded alveoli, down-regulation of caveolin-1, and increased expression of MT1-MMP, TIMP2, and the mature form of MMP2. Under resting conditions, there is hypoxia in many organs of ER$\beta^{-/-}$ mice, and this hypoxia becomes exaggerated when mice exercise on a treadmill. We suggest that lung dysfunction in ER$\beta^{-/-}$ mice induces systemic hypoxia, which can be involved in the heart hypertrophy (5) and systemic hypertension (6) observed in these mice.

Results

Phenotypic, Histological, and Immunohistochemical Examination of Lung Parenchyma in ER$\beta^{-/-}$ Mice. Hematoxylin/eosin-stained sections of lungs from 5-month-old WT mice look histologically normal (Fig. 1*A*). By 5 months of age (Fig. 1*B*), ER$\beta^{-/-}$ mouse lungs show large areas where alveoli are totally uninflated and septa are thickened. This age-related phenotype was evident to the same extent in both males and females but was not seen in WT littermates. Azan staining (Fig. 1 *C* and *D*) indicates

Conflict of interest statement: In addition to the partial funding of this study from Karo Bio AB, J.-Å.G. is a cofounder, deputy board member, stockholder, and consultant of Karo Bio AB.

Abbreviations: ER, estrogen receptor α; ER$\beta^{-/-}$, ERβ knockout; ECM, extracellular matrix; MMPs, matrix metalloproteinases; TIMPs, tissue inhibitors of metalloproteinases; MT1-MMP, membrane-type 1 metalloproteinase; HIF-1α, hypoxia-inducible factor 1α.

¶To whom correspondence should be addressed. E-mail: jan-ake.gustafsson@mednut.ki.se.

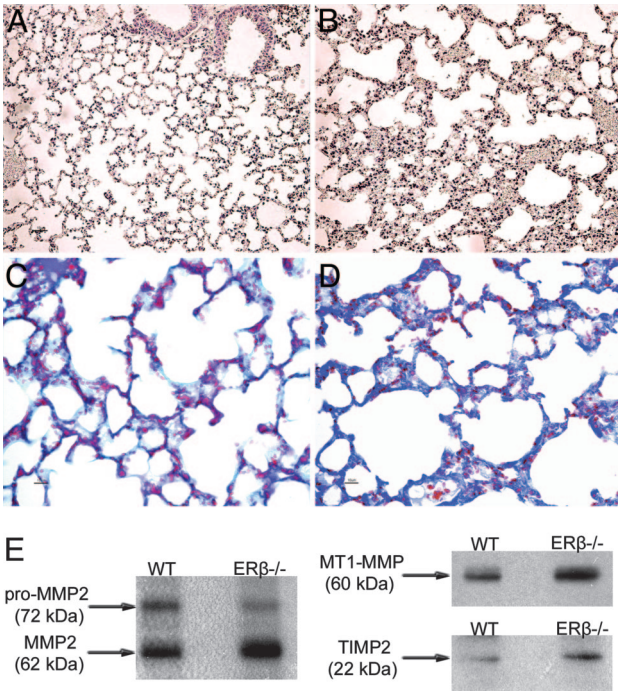

Fig. 1. Hematoxylin/eosin staining of lung from 1-year-old WT and ER$\beta^{-/-}$ mice. There is normal alveolar structure in WT lung sections (*A*), whereas areas of collapsed alveoli are evident in the ER$\beta^{-/-}$ lung sections (*B*). (*C*) Azan staining shows blue-stained collagenous extracellular material in the alveolar septa of WT lung section. (*D*) Intense blue-stained accumulation of ECM and thick alveolar septa in ER$\beta^{-/-}$ lung. (*E*) Immunoblotting of lung membrane fraction shows decreased ratio of inactive 72-kDa MMP2 form to the 62-kDa MMP2 active form and increased expression of MT1-MMP and TIMP2 in ER$\beta^{-/-}$ mice. (Magnification: *A* and *B*, ×10; *C* and *D*, ×20.)

substantial accumulation of collagen deposits in the alveolar septa of ER$\beta^{-/-}$ mice as confirmed in electron microscopic images (Fig. 2 *A–D*). Immunofluorescence revealed that expression of caveolin-1 was much lower in the lungs of ER$\beta^{-/-}$ mice than in their WT littermates (Fig. 3 *A–B*).

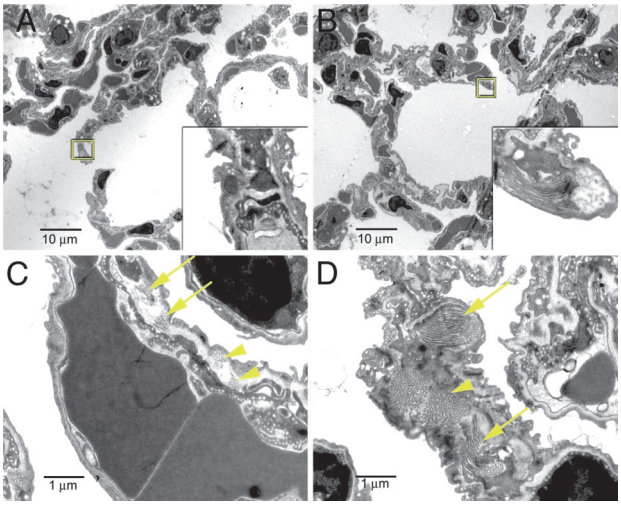

Fig. 2. EM of alveolar septa of WT and ER$\beta^{-/-}$ lung sections. Accumulation of collagen fibers are evident in ER$\beta^{-/-}$ lung septa (*B* and *D*) in longitudinal (arrows) and transversal (arrowheads) positions of the lung sections. In WT lung, collagen appears to be distributed in smaller and scattered fibers (*A* and *C*; arrows) than in ER$\beta^{-/-}$ lung.

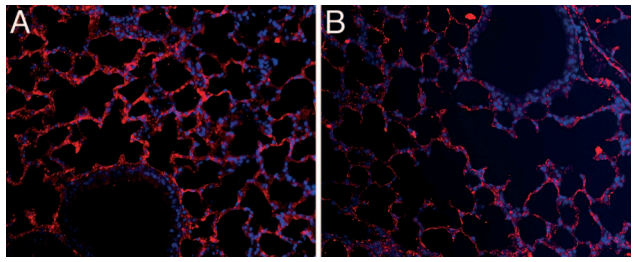

Fig. 3. Immunofluorscence staining for caveolin-1 shows down-regulation of this protein in the lungs of ER$\beta^{-/-}$ mice (*B*) compared with WT mice (*A*). (Magnification: ×20.)

Upon Western blotting with lung membrane fractions, two specific bands were detected with antibodies specific for MMP2. The 72-kDa band represents the inactive MMP2 and the 62-kDa band the proteolytically cleaved, active MMP2. Compared with WT littermates, in ER$\beta^{-/-}$ mice the ratio of the two bands is changed in favor of the smaller active protein (Fig. 1*E*). There are also increased levels of MT1-MMP, the protease involved in cleavage of MMP2, and TIMP2.

Hypoxic Organs in ER$\beta^{-/-}$ Mice. As represented in Fig. 4 *A–F*, expression of the hypoxia-inducible factor 1α (HIF-1α) in cardiomyocytes, epithelial cells of ventral prostate, and the periovarian sac is higher in ER$\beta^{-/-}$ mice than in WT littermates.

Hydroxyprobe is an exogenous nitroaromatic compound

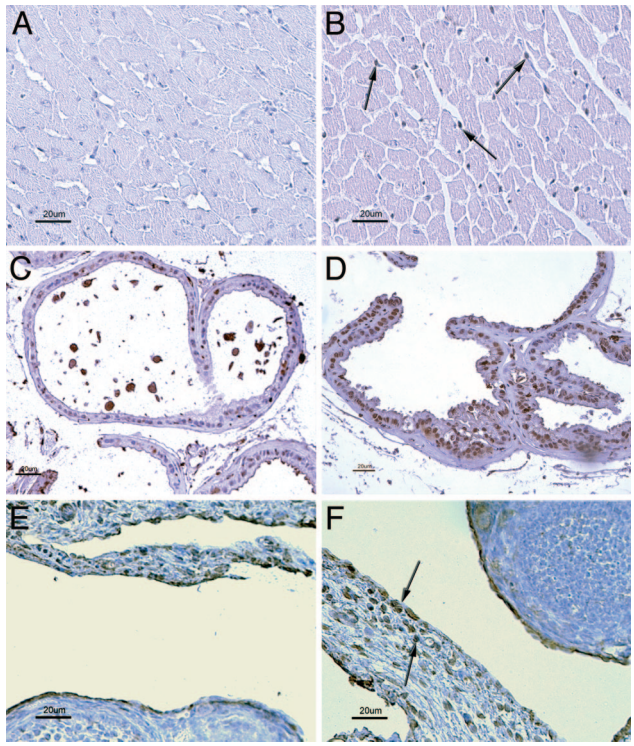

Fig. 4. Immunohistochemical detection of HIF-1α in heart, ventral prostate, and ovarian sac. There is no nuclear staining in the cardiomyocytes of WT mice (*A*). Several cells are positively stained in the nucleus in the heart section of ER$\beta^{-/-}$ mice (*B*). Very few weakly stained epithelial cell nuclei are found in the ventral prostate of WT mice (*C*), whereas almost the whole prostatic epithelium of ER$\beta^{-/-}$ mice is intensively stained (*D*). There are very strong positive signals in many cells of the periovarian sac in the ER$\beta^{-/-}$ mice (*F*) but only weakly stained cells in WT sections (*E*). There were no HIF-1α-positive cells in the ovary of either WT or ER$\beta^{-/-}$ mice. (Magnification: *A–D*, ×20; *E* and *F*, ×40.)

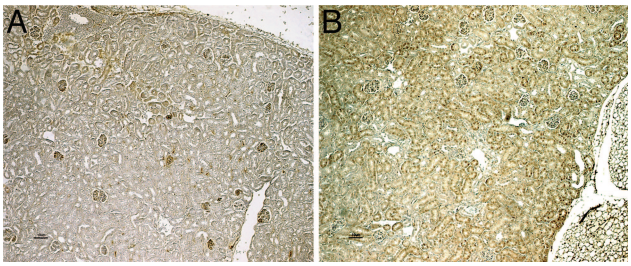

Fig. 5. Positive and negative controls for determination of the specificity of Hypoxyprobe. A generally stronger and more widely distributed positive signal is evident in the kidney sections of mice exposed to prolonged hypoxia (*B*) compared with mice exposed to normal air (*A*). (Magnification: ×10.)

[1-[(2-hydroxy-3-piperidinyl)propyl]-2-nitroimidazole hydrochloride] frequently used to study hypoxia in cancer (27–29). Hydroxyprobe is metabolized in a stepwise reduction pathway by cellular nitroreductase enzymes that are able to use the nitroaromatic compounds as alternative electron acceptors in case of low physiological level of pO_2 [$pO_2 < 10$ mmHg (1 mmHg = 133 Pa)]. The fragmentation of the imidazole ring leads to formation of reactive species, which form chemical adducts with several macromolecular components of cells (29, 30). Hypoxyprobe chemical adducts can be detected by a specific antibody by immunohistochemistry in hypoxic tissues (30). We tested the specificity of Hypoxyprobe staining on anesthetized 3-month-old WT mice exposed to prolonged hypoxia and mice breathing normal air (Fig. 5 *A* and *B*). Fig. 6 shows chemical adducts detected in various organs of ER$\beta^{-/-}$ and WT mice with Hypoxyprobe immunostaining. As shown in Fig. 6*A*, the liver is normally hypoxic (22) with positive cytoplasmic staining in areas close to the central veins in WT mice. In sections of ER$\beta^{-/-}$ mouse liver (Fig. 6*B*), the hepatocytes appear to be more strongly stained, and both the cytoplasm and nuclei are positive. In kidney sections of WT mice, there was also some cytoplasmic staining in tubular epithelial cells, but in ER$\beta^{-/-}$ mice, there was also very strong nuclear staining (Fig. 6 *C* and *D*). In brain sections, no positively stained neurons were found in WT mice but in ER$\beta^{-/-}$ mice (Fig. 6 *E* and *F*).

Intolerance to Physical Exercise of ER$\beta^{-/-}$ Mice. On a treadmill set at 10 m/min, 1-year-old male and female ER$\beta^{-/-}$ mice became exhausted after 4–5 min and could not be stimulated to run even with light prodding. Age-matched WT littermates continued to run for 10 min without showing signs of exhaustion.

Worsening of Hypoxia in ER$\beta^{-/-}$ Mice. Hypoxyprobe immunostaining done after exposure of the mice to the treadmill showed severe hypoxia in ER$\beta^{-/-}$ mice. In the livers of WT mice (Fig. 7*A*), there was weak cytoplasmic staining in hepatocytes that could not be distinguished from the staining in nonexercised WT mice. In sections from ER$\beta^{-/-}$ liver, there was intense nuclear and cytoplasmic staining throughout the entire organ (Fig. 7*B*). In the WT kidney, there was some strong nuclear and cytoplasmic staining in tubular epithelial cells after exercise (Fig. 7*C*), but in ER$\beta^{-/-}$ mice, most tubular epithelial cells were strongly stained in nucleus and cytoplasm (Fig. 7*D*). As is shown in Fig. 7 *E* and *D*, brains of exercised ER$\beta^{-/-}$ littermates show areas where many neurons are positively stained. Very few hypoxic neurons are present in the WT mouse brains.

Discussion

The primary function of the lung is gas exchange, and the structure of the pulmonary ECM is highly specialized to facilitate ventilation and gas diffusion. ECM refers to the basement membrane and interstitial connective tissue. The involvement of

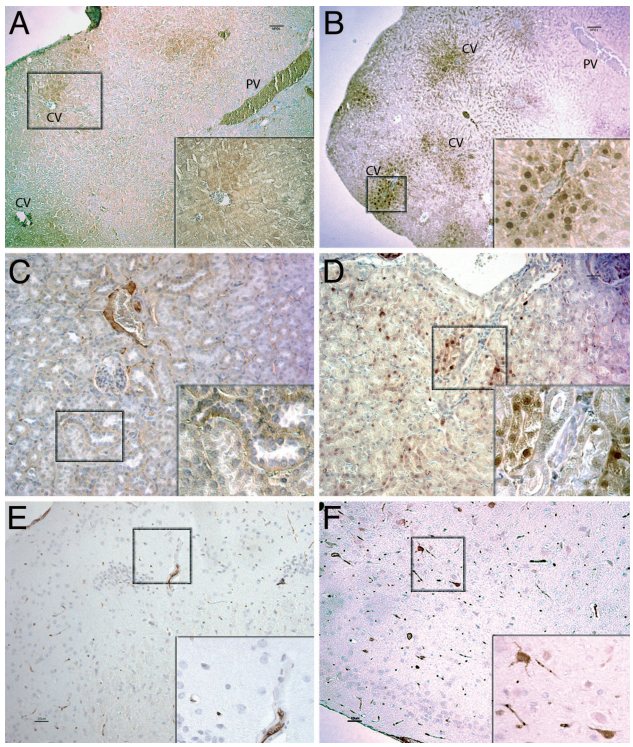

Fig. 6. Immunohistochemical detection of Hypoxyprobe chemical adducts. Liver and kidney are hypoxic organs. Hypoxia has been demonstrated in hepatocytes close to the central vein (CV) areas (31) . (*A*) In hepatocytes, there is a gradual increase in cytoplasmic staining from the portal veins (PV) toward the CV. (*B*) There is very strong nuclear and cytoplasmic staining in the hepatocytes of ER$\beta^{-/-}$ mice. (*C*) Positive cytoplasmic staining is seen in many tubular epithelial cells of the kidney of WT mice. (*D*) Stronger cytoplasmic staining and presence of some areas of nuclear staining in the kidney of ER$\beta^{-/-}$ mice. (*E*) No staining in the whole-brain section of WT mice (here represented as a supraopticus area). (*F*) Presence of some positively stained neurons in the brain of ER$\beta^{-/-}$ mice. (Magnification: *A* and *B*, ×10; *C–F*, ×20; *Inset*, ×40.)

ERβ in maintenance of lung ECM has already been hypothesized (12), but the role of ERβ has not been defined. In this article, we report that after 5 months of age ER$\beta^{-/-}$ mouse lungs are fibrotic, with loss of inflation and thickened septa. Azan staining and EM analysis showed evidence of accumulation of collagen in the ECM. By Western blotting analysis, there was more of the 62-kDa active fragment MMP2 than of the inactive 72-kDa protein. The increased activation of MMP2 is consistent with the finding of increased MT1-MMP and TIMP2 in the membrane fraction of the lung of ER$\beta^{-/-}$ mice.

It has been demonstrated that MMP2 activation occurs by proteolytic activity of the complex formed by MT1-MMP and TIMP2 (20). Studies on MT1-MMP knockout mice indicate that this enzyme is important for normal alveolar development, independent of its ability to activate MMP2 (32). However, overexpression and overactivation of MMP2 is associated with several pulmonary pathologies. For instance, excessive MMP2 and MMP9 production detected in fibrotic lung is thought to play a role in the disruption of basal membrane and consequent triggering of tissue-remodeling process (33). Our results show that ERβ has some important function in the regulation of expression of the complex MT1-MMP–TIMP2 and therefore also of MMP2 activity.

Our finding of down-regulation of caveolin-1 in the lungs of ER$\beta^{-/-}$ mice indicates another possible mechanism by which ERβ can be involved in the maintenance of the ECM in the lung. Dysregulation of caveolin-1 expression can lead to dispersion of

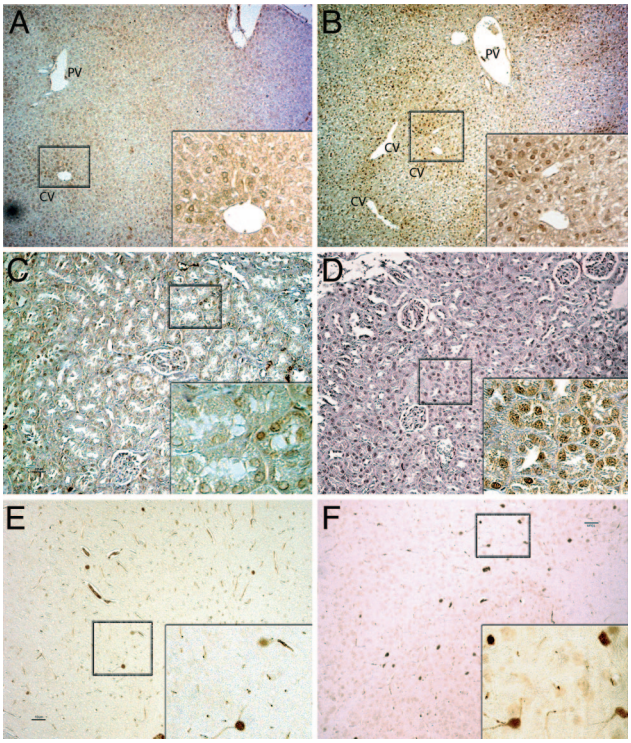

Fig. 7. Immunohistochemical detection of Hypoxyprobe chemical adducts in mice killed after physical strain on a treadmill (speed, 10 m/min). (*A*) A weak cytoplasmic signal is evident in the hepatocytes close to the central vein (CV) in WT mice. PV, portal veins. (*B*) Extended regions of strong cytoplasmic and nuclear staining in the liver of ER$\beta^{-/-}$ mice. (*C*) Some tubular epithelial cells are stained in both cytoplasm and nucleus of WT kidney, whereas most cells show only cytoplasmic signal. (*D*) Almost the entire epithelial tubular cell of the kidney of ER$\beta^{-/-}$ mice shows strong positive signals in both cytoplasm and nucleus. (*E*) There are very few stained neurons in brain section of WT mice. (*F*) There are many areas with stained neurons in the section of ER$\beta^{-/-}$ mice. (Magnification: *A* and *B*, ×10; *C–F*, ×20; *Inset*, ×40.)

MT1-MMP from the lipid rafts of the plasma membrane, and this can interfere with several of the enzymatic activities of MT1-MMP (21). We speculate that ERβ regulates both the expression of MT1-MMP and its localization on the lipid rafts of the plasma membrane. Physiologically, there is a balance between deposition and degradation of the ECM and disruption of this balance leads to lung-fibrotic diseases or impaired wound-healing (34). MMP activities are responsible for maintenance of ECM.

Immunohistochemical analysis of HIF-1α and Hypoxyprobe chemical adducts revealed several hypoxic organs in ERβ knockout mice (Fig. 5). In our experimental setting, 1-year-old ER$\beta^{-/-}$ mice were much less tolerant to physical strain on a treadmill than were WT littermates: ERβ-deficient mice ''refused'' to run for >5 min, whereas WT mice could continue to run up to 10–15 min. Hypoxyprobe staining shows that (Fig. 6), after exercise, hypoxia in liver, kidney, and brain was much more severe in the ER$\beta^{-/-}$ than WT mice. The intolerance of ER$\beta^{-/-}$ mice to physical exercise may be due to systemic hypoxia caused by lung dysfunction.

In conclusion, ER$\beta^{-/-}$ mice have abnormal alveolar structure, abnormal ECM composition, and dysregulation of MMP2, MT1-MMP, TIMP2, and caveolin-1. The chronic hypoxia of ER$\beta^{-/-}$ mice must be considered as a contributing factor in other abnormalities in these mice, including hypertension that develops in both male and female ER$\beta^{-/-}$ mice after 6 months of age (6). Systemic hypertension is associated with peripheral vasoconstriction, which can be caused by several factors, including adaptations to chronic hypoxia (35, 36). The creation of tissue-specific knockout mice may be very useful to study the role of ERβ in the cardiovascular system and other tissues, avoiding the secondary effects due to systemic hypoxia.

Materials and Methods

Animals. ER$\beta^{-/-}$ mice were from our colony (4). Mice were housed in the Karolinska University Hospital Animal Facility (Huddinge, Sweden) in a controlled environment on a 12-h light/dark illumination schedule and fed a standard pellet diet with water provided ad libitum. Mice were killed by cervical dislocation and exsanguinated by cutting of the abdominal aorta. For immunohistochemical studies, lungs were fixed in 4% paraformaldehyde and embedded in paraffin; for Western blotting, lungs were frozen in liquid nitrogen.

Physical Strain Test. One group of 1-year-old male and female ER$\beta^{-/-}$ mice and another group of male and female WT mice of the same age were subjected to physical exercise on a treadmill set at the speed of 10 m/min.

Western Blotting. The lung membrane fractions of ER$\beta^{-/-}$ and WT mice were analyzed by Western blotting with antibodies raised against MMP2, MT1-MMP, and TIMP-2. Frozen tissues were homogenized for 1 min each with a polytron in 25 ml of PBS buffer containing a protease inhibitor mixture according to manufacturer's instructions (Roche Diagnostics). The homogenate was centrifuged for 10 min at 1,000 rpm (rotor JA-17; Beckman). The pellet contained nuclear protein, and the supernatant contained mitochondrial, cytosolic, and membrane proteins. Mitochondrial proteins were precipitated and removed by centrifugation of the supernatant at 9,000 rpm for 20 min (rotor JA-17). After ultracentrifugation at 30,000 rpm for 60 min (rotor Ti50; Beckman), membrane proteins were precipitated and resuspended in PBS. The membrane proteins of WT and ER$\beta^{-/-}$ mice lung were dissolved in SDS sample buffer and resolved on 4–20% gradient SDS/polyacrylamide gels (Invitrogen) in Tris-glycine buffer. The protein contents of the lanes were compared by Coomassie blue staining of the gel. The same amount of proteins were loaded on another gel and then transferred to poly(vinylidene difluoride) membranes (Amersham Pharmacia Biosciences) by electroblotting in Tris-glycine buffer. Molecular weight markers were Precision Plus protein standards (Bio-Rad). The membrane was then incubated in blocking solution containing 5% fat-free milk and 0.1% Nonidet P-40 in PBS for 1 h at room temperature. Incubations with mouse anti-MMP2, mouse anti-MT1-MMP, or rabbit anti-TIMP2 antibodies were performed in blocking solution overnight at 4°C. After washing, secondary peroxidase-conjugated goat anti-mouse or anti-rabbit antibodies (1:3,000; Sigma) were applied in blocking solution for 1 h at room temperature. After washing, detection with an enhanced chemiluminescence ECL kit (Amersham Pharmacia) was performed.

EM. Lungs were dissected, and small pieces were cut and immediately fixed in 2% glutaraldehyde/0.5% paraformaldehyde in 0.1 M sodium cacodylate buffer (caco)/0.1 M sucrose/3 mM $CaCl_2$ (pH 7.4) overnight. Specimens were rinsed in 0.15 M caco and postfixed by incubation for 2 h in 2% osmium tetroxide in 0.07 M caco containing 3 mM $CaCl_2$. The specimens were dehydrated in an ascending series of alcohol into acetone and embedded in LX-112 epoxy resin (Ladd Research Industries, Burlington, VT). Semithin sections (0.5 μm) were placed on glass slides, stained with toluidine blue, and examined in a light microscope. Ultrathin sections were cut and contrasted with uranyl acetate followed by lead citrate and examined in a Tecnai 10 (FEI, Eindhoven, The Netherlands) transmission electron microscope set at 80 kV.

Tissue Hypoxia Detection by a Hypoxyprobe Kit. Hypoxyprobe solution was injected 60 mg/kg i.p. 15 min before the running test. The animals were killed just after the physical strain. For the mice not exposed to physical exercise, the Hypoxyprobe treatment was done 60 min before death.

Immunohistochemistry. Representative blocks of paraffin-embedded tissues were cut at a 4-μm thickness, dewaxed, and rehydrated. For all of the stainings, the antigens were retrieved by boiling in 10 mM citrate buffer (pH 7.0) for 20 min. In the case of HIF-1α and Hypoxyprobe stainings, the sections were incubated in 0.5% H_2O_2 in PBS for 30 min at room temperature to quench endogenous peroxidase and then incubated in 0.5% Triton X-100 in PBS for 30 min. To block the nonspecific binding, sections were incubated in 1% BSA plus 0.1% Nonidet P-40 in PBS for 1 h at 4°C. Sections were incubated with mouse anti-HIF-1α or mouse anti-Hypoxyprobe antibodies, both at a dilution of 1:50 in 1% BSA and 0.1% Nonidet P-40 in PBS overnight at 4°C. After washing, sections were incubated with the secondary antibodies (biotinylated goat IgG anti-mouse for HIF-1α and biotinylated goat IgG F(ab′)$_2$ anti-mouse for Hypoxyprobe) for 1 h at room temperature. The Vectastain ABC kit (Vector Laboratories) was used for the avidin–biotin complex (ABC) method according to the manufacturer's instructions. Peroxidase activity was visualized with 3,3′-diaminobenzidine (DAKO). The sections were lightly counterstained with hematoxylin or DAPI, dehydrated through an ethanol series to xylene, and mounted. For caveolin-1 staining, the sections were incubated with rabbit anti-caveolin-1 in 3% BSA plus 0.1% Nonidet P-40 in PBS overnight at 4°C. After washing, sections were incubated with goat Cy3 anti-rabbit antibody. The sections were then dehydrated and directly mounted in Vectashield antifading medium (Vector Laboratories). The visualizations were done by using a light microscope or Zeiss fluorescence microscope with filters suitable for selectively detecting the fluorescence of Cy3 (red).

Chemicals and Antibodies. We purchased DAPI from Sigma–Aldrich and the Hypoxyprobe Kit from Chemicon International (Temecula, CA). The following antibodies were used: mouse monoclonal anti-HIF-1α from Chemicon International, mouse monoclonal anti-MMP2 from Zymed, mouse monoclonal anti-MT1-MMP from Chemicon International, rabbit polyclonal anti-TIMP2 from Abcam, Inc. (Cambridge, MA), rabbit polyclonal anti-caveolin-1 from BD Biosciences, Cy3 anti-rabbit from Jackson ImmunoResearch, and biotinylated goat IgG anti-mouse and biotinylated goat F(ab′)$_2$ IgG from Zymed.

We thank Annemarie Witte and José Inzunza for excellent technical assistance and animal management. This work was supported by the European Commission funded CASCADE Network of Excellence (FOOD-CT-2004-506319), the Swedish Cancer Fund, and Karo Bio AB (Huddinge, Sweden).

1. Ballard, P. L. (1989) *Endocr. Rev.* **10,** 165–181.
2. Mendelson, C. R. & Boggaram, V. (1990) *Baillieres Clin. Endocrinol. Metab.* **4,** 351–378.
3. Kuiper, G. G., Enmark, E., Pelto-Huikko, M., Nilsson, S. & Gustafsson, J. A. (1996) *Proc. Natl. Acad. Sci. USA* **93,** 5925–5930.
4. Krege, J. H., Hodgin, J. B., Couse, J. F., Enmark, E., Warner, M., Mahler, J. F., Sar, M., Korach, K. S., Gustafsson, J. A. & Smithies, O. (1998) *Proc. Natl. Acad. Sci. USA* **95,** 15677–15682.
5. Forster, C., Kietz, S., Hultenby, K., Warner, M. & Gustafsson, J. A. (2004) *Proc. Natl. Acad. Sci. USA* **101,** 14234–14239.
6. Zhu, Y., Bian, Z., Lu, P., Karas, R. H., Bao, L., Cox, D., Hodgin, J., Shaul, P. W., Thoren, P., Smithies, O., *et al.* (2002) *Science* **295,** 505–508.
7. Cheng, G., Weihua, Z., Makinen, S., Makela, S., Saji, S., Warner, M., Gustafsson, J. A. & Hovatta, O. (2002) *Biol. Reprod.* **66,** 77–84.
8. Imamov, O., Morani, A., Shim, G. J., Omoto, Y., Thulin-Andersson, C., Warner, M. & Gustafsson, J. A. (2004) *Proc. Natl. Acad. Sci. USA* **101,** 9375–9380.
9. Forster, C., Makela, S., Warri, A., Kietz, S., Becker, D., Hultenby, K., Warner, M. & Gustafsson, J. A. (2002) *Proc. Natl. Acad. Sci. USA* **99,** 15578–15583.
10. Wada-Hiraike, O., Imamov, O., Hiraike, H., Hultenby, K., Schwend, T., Omoto, Y., Warner, M. & Gustafsson, J. A. (2006) *Proc. Natl. Acad. Sci. USA* **103,** 2959–2964.
11. Patrone, C., Cassel, T. N., Pettersson, K., Piao, Y. S., Cheng, G., Ciana, P., Maggi, A., Warner, M., Gustafsson, J. A. & Nord, M. (2003) *Mol. Cell. Biol.* **23,** 8542–8552.
12. Massaro, D. & Massaro, G. D. (2004) *Am. J. Physiol.* **287,** L1154–L1159.
13. Arden, M. G., Spearman, M. A. & Adamson, I. Y. (1993) *Am. J. Respir. Cell Mol. Biol.* **9,** 99–105.
14. Reponen, P., Sahlberg, C., Huhtala, P., Hurskainen, T., Thesleff, I. & Tryggvason, K. (1992) *J. Biol. Chem.* **267,** 7856–7862.
15. Fukuda, Y., Ishizaki, M., Okada, Y., Seiki, M. & Yamanaka, N. (2000) *Am. J. Physiol.* **279,** L555–L561.
16. Atkinson, J. J., Holmbeck, K., Yamada, S., Birkedal-Hansen, H., Parks, W. C. & Senior, R. M. (2005) *Dev. Dyn.* **232,** 1079–1090.
17. Masumoto, K., de Rooij, J. D., Suita, S., Rottier, R., Tibboel, D. & de Krijger, R. R. (2005) *Histopathology* **47,** 410–419.
18. Parks, W. C. & Shapiro, S. D. (2001) *Respir. Res.* **2,** 10–19.
19. Elkington, P. T. & Friedland, J. S. (2006) *Thorax* **61,** 259–266.
20. Corbel, M., Belleguic, C., Boichot, E. & Lagente, V. (2002) *Cell Biol. Toxicol.* **18,** 51–61.
21. Henry, M. T., McMahon, K., Mackarel, A. J., Prikk, K., Sorsa, T., Maisi, P., Sepper, R., Fitzgerald, M. X. & O'Connor, C. M. (2002) *Eur. Respir. J.* **20,** 1220–1227.
22. Butler, G. S., Butler, M. J., Atkinson, S. J., Will, H., Tamura, T., van Westrum, S. S., Crabbe, T., Clements, J., d'Ortho, M. P. & Murphy, G. (1998) *J. Biol. Chem.* **273,** 871–880.
23. Annabi, B., Lachambre, M., Bousquet-Gagnon, N., Page, M., Gingras, D. & Beliveau, R. (2001) *Biochem. J.* **353,** 547–553.
24. Rothberg, K. G., Heuser, J. E., Donzell, W. C., Ying, Y. S., Glenney, J. R. & Anderson, R. G. (1992) *Cell* **68,** 673–682.
25. Drab, M., Verkade, P., Elger, M., Kasper, M., Lohn, M., Lauterbach, B., Menne, J., Lindschau, C., Mende, F., Luft, F. C., *et al.* (2001) *Science* **293,** 2449–2452.
26. Barros, R. P., Machado, U. F., Warner, M. & Gustafsson, J. A. (2006) *Proc. Natl. Acad. Sci. USA* **103,** 1605–1608.
27. Cline, J. M., Thrall, D. E., Page, R. L., Franko, A. J. & Raleigh, J. A. (1990) *Br. J. Cancer* **62,** 925–931.
28. Raleigh, J. A., Calkins-Adams, D. P., Rinker, L. H., Ballenger, C. A., Weissler, M. C., Fowler, W. C., Jr., Novotny, D. B. & Varia, M. A. (1998) *Cancer Res.* **58,** 3765–3768.
29. Hodgkiss, R. J. (1998) *Anticancer Drug Des.* **13,** 687–702.
30. Kennedy, A. S., Raleigh, J. A., Perez, G. M., Calkins, D. P., Thrall, D. E., Novotny, D. B. & Varia, M. A. (1997) *Int. J. Radiat. Oncol. Biol. Phys.* **37,** 897–905.
31. Samoszuk, M. K., Walter, J. & Mechetner, E. (2004) *J. Histochem. Cytochem.* **52,** 837–839.
32. Oblander, S. A., Zhou, Z., Galvez, B. G., Starcher, B., Shannon, J. M., Durbeej, M., Arroyo, A. G., Tryggvason, K. & Apte, S. S. (2005) *Dev. Biol.* **277,** 255–269.
33. Chakrabarti, S. & Patel, K. D. (2005) *Exp. Lung Res.* **31,** 599–621.
34. Razzaque, M. S. & Taguchi, T. (2003) *Pathol. Int.* **53,** 133–145.
35. Vaziri, N. D. & Wang, Z. Q. (1996) *Kidney Int.* **49,** 1457–1463.
36. Calbet, J. A. (2003) *J. Physiol.* **551,** 379–386.